J Mater Sci (2010) 45:1220–1226
DOI 10.1007/s10853-009-4068-5

An etching characterization method for revealing the plastic deformation zone in a SUS303 stainless steel

Mitsuhiro Okayasu · Kazuto Sato · Satoshi Takasu

Received: 28 July 2009 / Accepted: 22 November 2009 / Published online: 9 December 2009

Abstract Etching characteristics used to reveal localized plastic deformation zones in a SUS303 stainless steel have been examined. The etching was conducted on a sample using an etchant consisting of 5-g ferric chloride, 50-mL hydrochloric acid, and 100-mL water. The sample was deformed severely and heated to various temperatures before the etching process. With this etching technique, the plastically deformed area is clearly observed even at low magnification. This is due to a change of the microstructural characteristics in the plastic deformation zone. There are different microstructure patterns that reveal the plastic zone in the sample with and without heating, e.g., plastic zone in the sample with heating to 800 °C is observed clearly due to randomly oriented crystals and recrystallized small grains with precipitated nano-size particles. Details of the etching characteristics that reveal the plastic deformation zone are further discussed.

Introduction

It is reported that more than 90% of component failures are caused by fatigue, and the fatigue strength is attributed directly to the crack growth rate. The crack growth speed is associated with the severity of plastic deformation around the crack tip. In recent years, the effect of plastic deformation on the crack growth characteristic has been extensively studied. Many researchers have investigated the deformation characteristics using various experimental techniques, such as etching techniques, photoelastic stress analysis, and microhardness measurements. Due to its accuracy, simplicity, and low cost, etching is a very suitable approach for observing the plastic deformation zone.

Such etching techniques have been reported by Fry [1] and Morris [2]. With their techniques, the plastically deformed area in mild steels can be identified from the segregation of impurity atoms at dislocation cores, where etch-pit formation occurs. Applications of their techniques can be found in many published reports [3–6], e.g., the plastic deformation zone in specimens of Fe-3%Si steels subjected to bending is revealed clearly [5, 6]. Moreover, Frühauf et al. [7] have examined the characteristic of plastic behavior in silicon microelements by etch-pit technique. Meguid [8] reported that plastically deformed regions in aluminum can be revealed by an etching technique using a solution modified from Tucker's etchant [9]. Some etching methods have been developed several decades ago for revealing plastic deformation zones but there are apparently material limitations. In fact, few metals are suitable in this way. To extend the etching technology, the authors propose alternative etching techniques. With these, the plastic deformation zones in several materials can be clearly delineated [10–13], these include carbon steels, Al alloys and Mg alloys. The concept of our etching technique is to alter the microstructure in the deformation zone by a heating process.

Stainless steels have been served widely in various structures and components, e.g., power plant pipes and automotive parts [14]. This is because of its combination of acceptable strength, superior ductility, and high oxidation resistance. Those components are produced by stretching, drawing, and bending, which causes severe plastic deformation in the alloys. Experimental and numerical approaches have been carried out to understand the stress–strain

M. Okayasu (✉) · K. Sato · S. Takasu
Department of Machine Intelligence and Systems Engineering, Akita Prefectural University, 84-4 Ebinokuchi, Tsuchiya-aza, Yurihonjo-City, Akita 015-0055, Japan
e-mail: okayasu@akita-pu.ac.jp

characteristics in stainless steels [15, 16]. Although an examination of the deformation characteristics of stainless steel is significant, no clear etching technique has been reported which reveals the plastic deformation zones. Therefore, the purpose of this study is to demonstrate an etching technique to observe the localized plastic deformation zone in stainless steels. In addition, an attempt has been made to investigate the detailed etching characteristics that reveal the plastic deformation zone.

Experimental

Material and experimental procedures

In this study, a SUS303 stainless steel was used. The chemical composition of the stainless steel is (wt%): 8 Ni, 18 Cr, and 0.2 S, balanced with Fe. The tensile properties of the material at room temperature are 0.2% proof strength $\sigma_{0.2} = 205$ MPa, tensile strength $\sigma_{UTS} = 520$ MPa, and elongation $\varepsilon_f = 40\%$. A severe plastic deformation was introduced by imposing a hardened high carbon steel wire (700 HV) with diameter 1.0 mm at a compressive force of 10 kN. The specimen was machined into the form of a rectangular block (10 mm × 10 mm × 5 mm). An electro-servo-hydraulic system with a capacity of 200 kN was employed to carry out the compressive loading. To investigate the etching characteristics that could identify the plastic deformation zone, the deformed samples were heated to different temperatures, e.g., 500, 650, and 800 °C for 1 h (Table 1). The choice of the heating temperatures is determined based upon the recrystallization temperature of this stainless steel, which is over 750 °C. The heating is used to distinguish the plastic deformation zone, since more severe precipitation occurs in the deformed area [10]. The etching technique proposed in this study is briefly summarized as follows: (i) the specimens are compressed to produce a severe plastic deformation, (ii) the deformed samples are heated to different temperatures, (iii) the specimen surface to be observed is ground to a mirror finish, (iv) the polished surface is etched for 30 s using an etchant consisting of 5-g $FeCl_3$, 50-mL HCl, and 100-mL H_2O. The microstructural observations were conducted using an optical microscope, with X-ray diffraction (XRD), and an electron back scatter diffraction analysis (EBSD). The fundamentals of the EBSD techniques employed in this study are described by Randle [17].

Table 1 Test samples

Sample A	Sample B	Sample C	Sample D
No heating	500 °C	650 °C	800 °C

Finite element analysis

To investigate the plastic strain distribution in the stainless steel sample after compressive loading, finite element analysis (FEA) was conducted using ANSYS software. In this analysis, a two-dimensional finite element simulation with 8-node quad elements was employed. A FEA model was designed based on the compression test, as described in the previous section. The mesh size of the area surrounding the hardened steel wire was 0.05 mm, where a

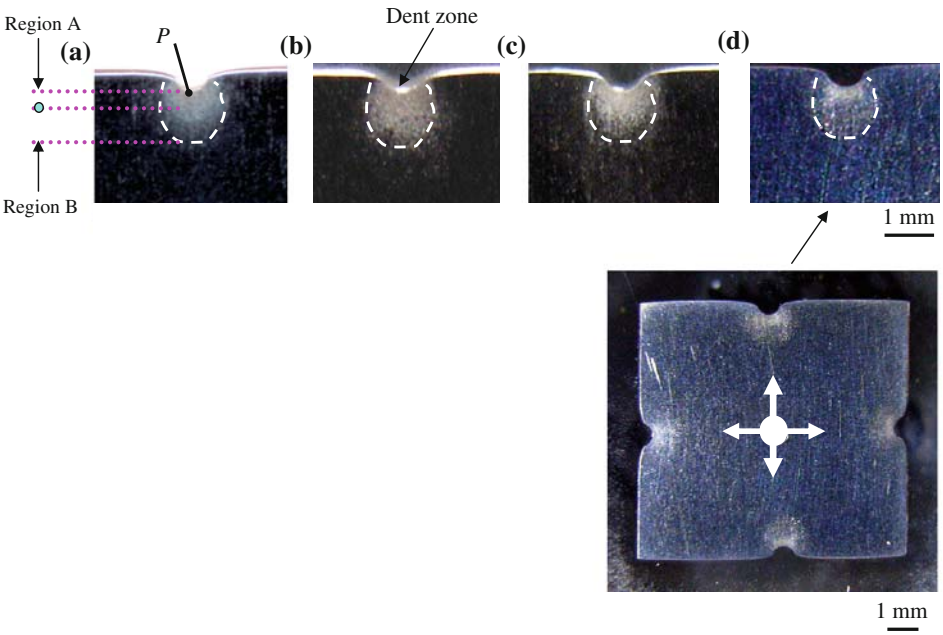

Fig. 1 Optical macrographs of SUS303 after etching: **a** no heating, **b** sample heated to 500 °C, **c** sample heated to 650 °C and **d** sample heated to 800 °C

total of 3,251 quadrilateral solid elements were used. Due to the high hardness of the steel wire when compared to the stainless steel, the hardened wire was considered to be rigid in this analysis. To model the contact between the hardened wire and the stainless steel sample, the area contact element (CONTACT 172 and TARGET 169 [18]) was used, corresponding to the geometry mesh of the model. The case of bilinear kinematic hardening was selected in this analysis, where the initial slope of the stress–strain curve is taken as Young's modulus of the material, and after material yield the curve continues along the second slope defined by the tangent modulus. The following material properties were employed: Young's modulus $E = 190$ GPa, tangent modulus $T = 19$ GPa, Poisson's ratio $v = 0.3$ and 0.2%, proof stress $\sigma_{0.2} = 205$ MPa.

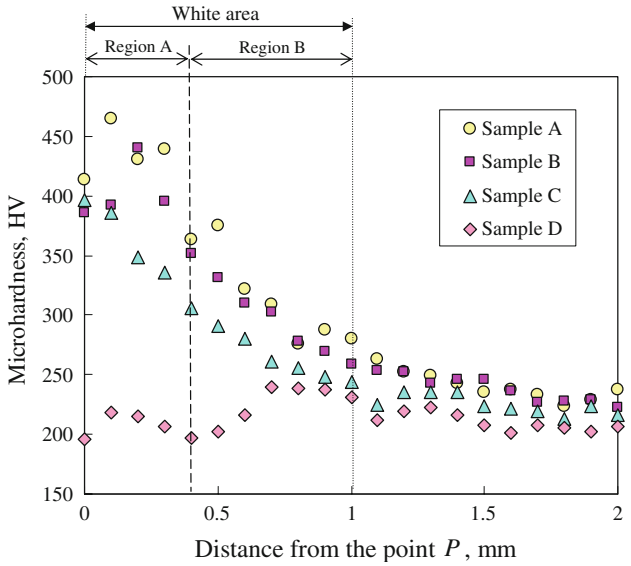

Fig. 2 Microhardness results from Samples A, B, C, and D measured from position *P*, as shown in Fig. 1a

Results and discussion

Figure 1 shows the macrostructure of the etched samples in the area adjacent to the dented zone. A round bright (white) region in the vicinity of the dented zone was observed for all the samples. The brightness is altered depending on the discolored area: strong brightness zone can be seen in the sample near the loading point, e.g., Region A versus Region B, see Fig. 1a. Moreover, the overall brightness of the sample heated to 800 °C is slightly weaker than that for the other samples, i.e., Samples A, B, and C versus Sample D. The reason for the weakness for Sample D will be discussed in a later section of this article. It should be noted that the white regions corresponded to severe etching [10]. Because of the lighting conditions, they appear white in the photographs taken by a digital camera. It is considered that the profile of the white areas in Fig. 1 can be attributed to the plastic deformation zone. To verify this, microhardness measurements in the bright and dark regions for all the samples were carried out. The hardness was measured in both the white and the dark areas from point *P*, as shown in Fig. 1a and the results obtained given in Fig. 2. As seen, the overall hardness in the white area is higher than that in the dark area for Samples A, B, and C even though the hardness level decreases even in the white zone (Region A vs. B). Such a high hardness in the bright zone suggests that the discolored area on the etched surface for Samples A–C reflects the actual plastic deformation zone (or work hardening area). The reason for the decrease of hardness in the white areas would then be related to the degree of brightness around the dented zone in Fig. 1, with the brighter the area, the higher the hardness. It is also seen that the hardness level in the white area for Samples A, B, and C is different depending on the heating temperature, with the lower the temperature, the higher the hardness. This may be attributed to softening of the sample because of heating. On the other hand, the hardness level in the white

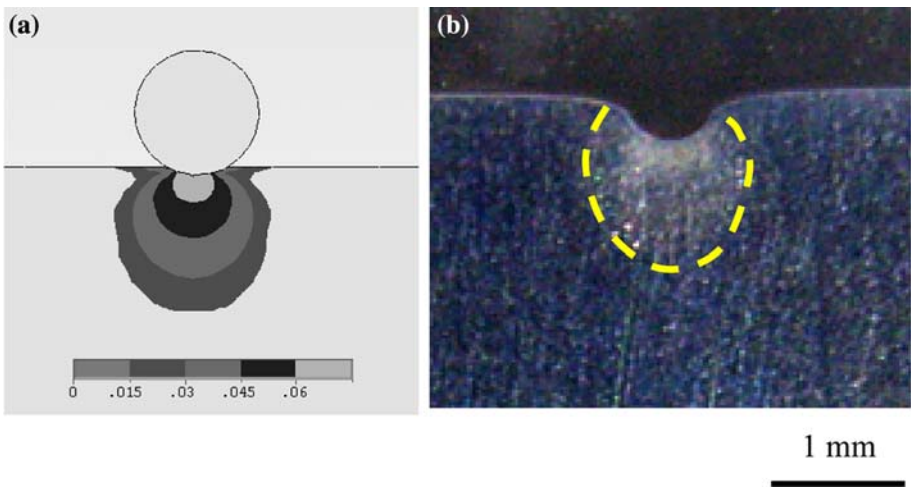

Fig. 3 **a** von-Mises plastic strain distribution obtained by an FE analysis; **b** optical macrograph of Sample D, showing the plastic deformation zone enclosed by the dashed line

region for Sample D is the same as for its dark area. Although the reason for the low hardness in the white area of Sample D can be considered to be due to the material softening or recrystallization, the reason for revealing of the bright zone is not yet clear and will be discussed later. To confirm the relationship between the plastic deformation zone and the white areas for Samples A, B, and C, the stress–strain distribution was examined using FE analysis. Figure 3a presents the von-Mises plastic strain distribution for the stainless steel sample. As can be seen, the shape of the plastic strain distribution is similar to the bright zone shown in Fig. 3b. This result convinces us that the white area for Samples A–C is associated with the actual plastic deformation.

To understand the mechanism behind the revealing of the plastic deformation zones, the microstructural characteristics of the samples were investigated. Figure 4 shows the microstructure of the undeformed and deformed zones of Samples A, B, C, and D. It can be seen that austenitic phases with f.c.c. crystal structures are obtained in the undeformed areas for all the samples. In Samples A–C, many slip bands (share bands) are detected in the plastic

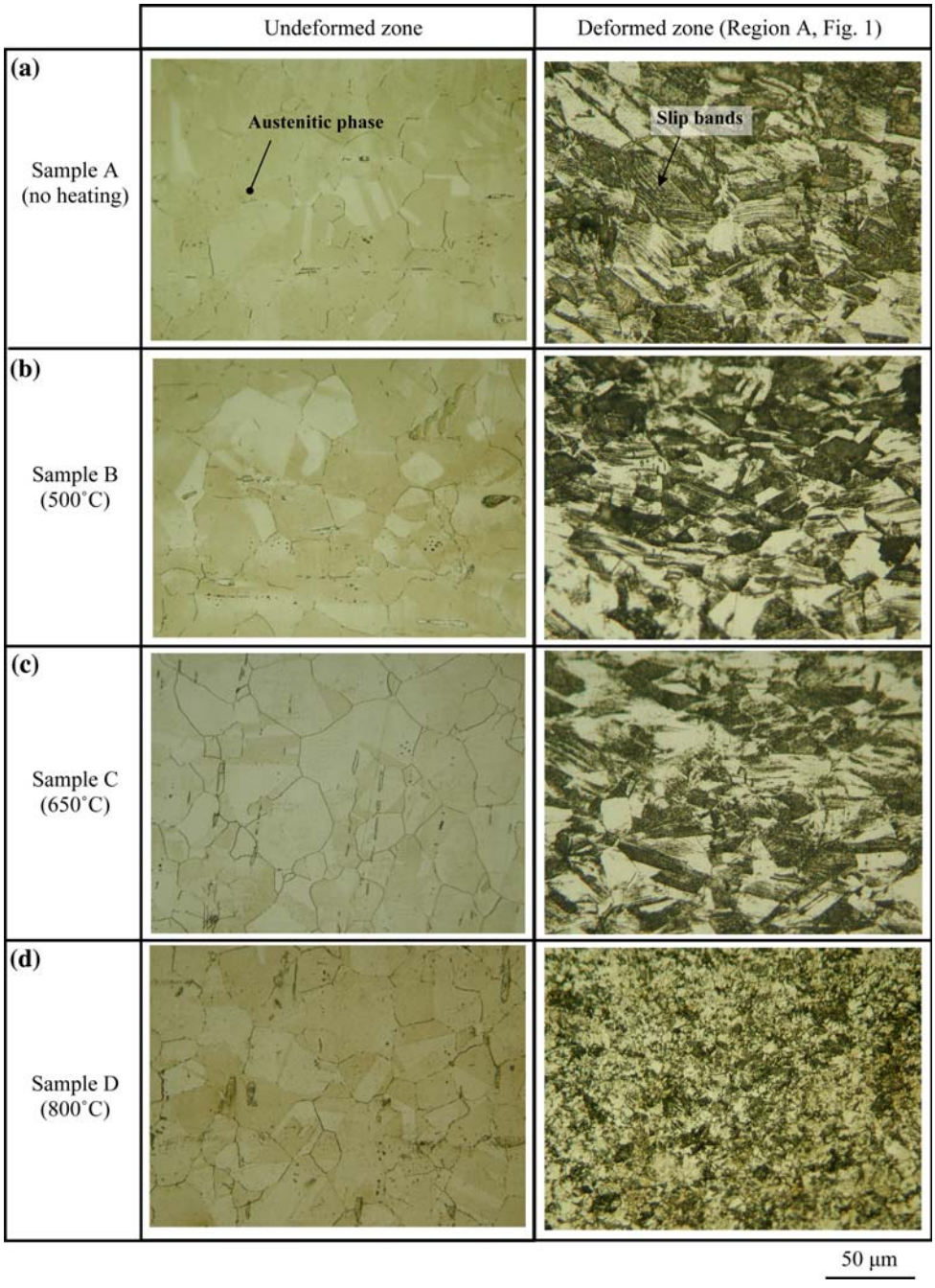

Fig. 4 Optical micrographs of undeformed and deformed regions

deformation zone near the loading point (*P*). Furthermore, the density of the slip band decreases in the area far from the point *P*, e.g., in Region B, as shown in Fig. 5a. Such a slip system is attributed to the high material hardness [19] (Fig. 2). In this case, the slip would have occurred on the close-packed {111} planes and in the ⟨110⟩ close-packed directions [15]. On the other hand, the microstructural formation in the deformation zone of Sample D is different, with small grains created by the heating process. Moreover, from the secondary electron image of the deformation zone

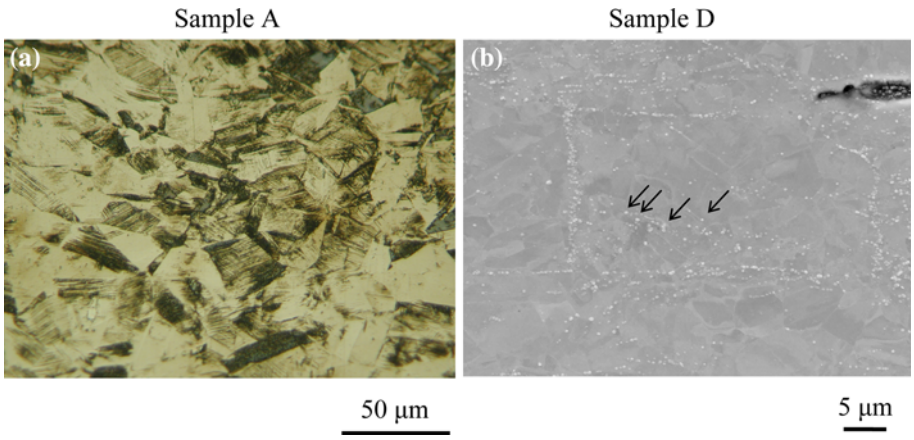

Fig. 5 Optical micrographs and secondary electron images of the deformed regions (Region B Fig. 1a) for Samples A and D

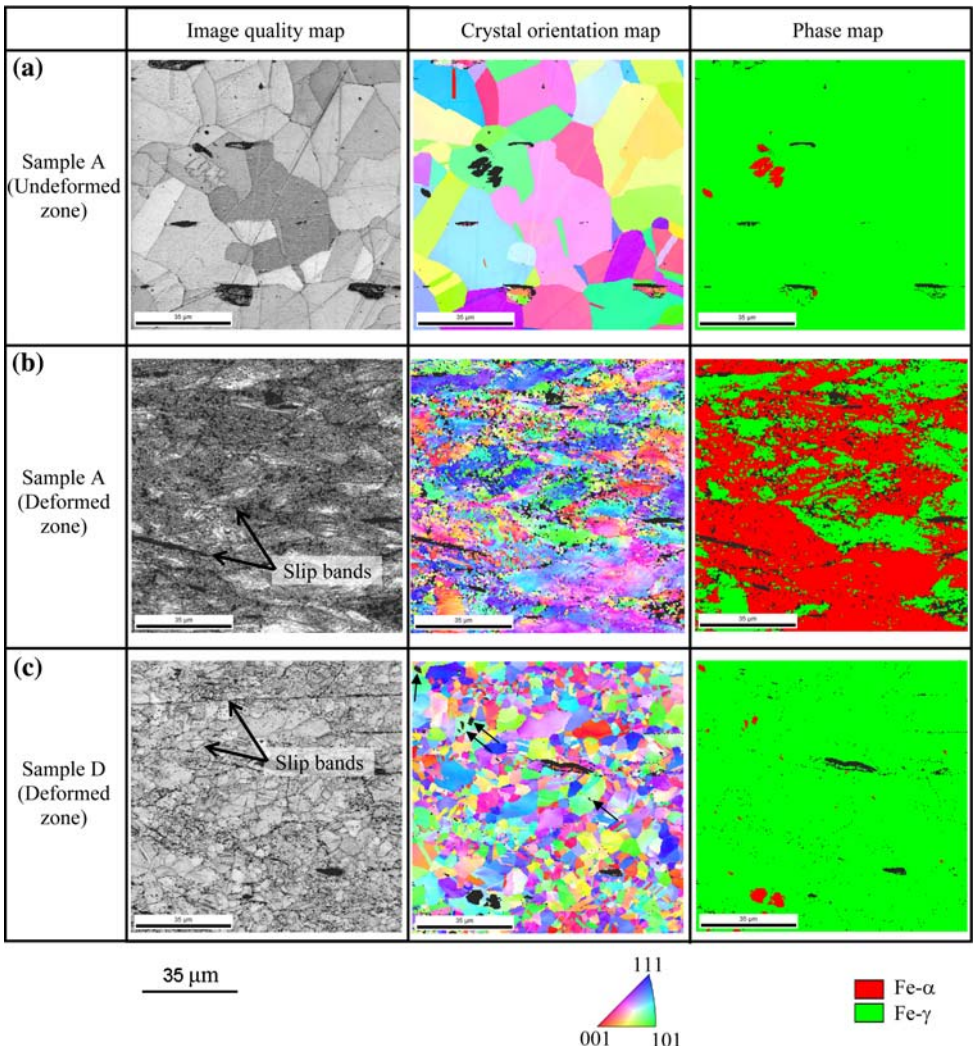

Fig. 6 EBSD analysis of Samples A and D, showing image-quality map, crystal-orientation map, and phase map

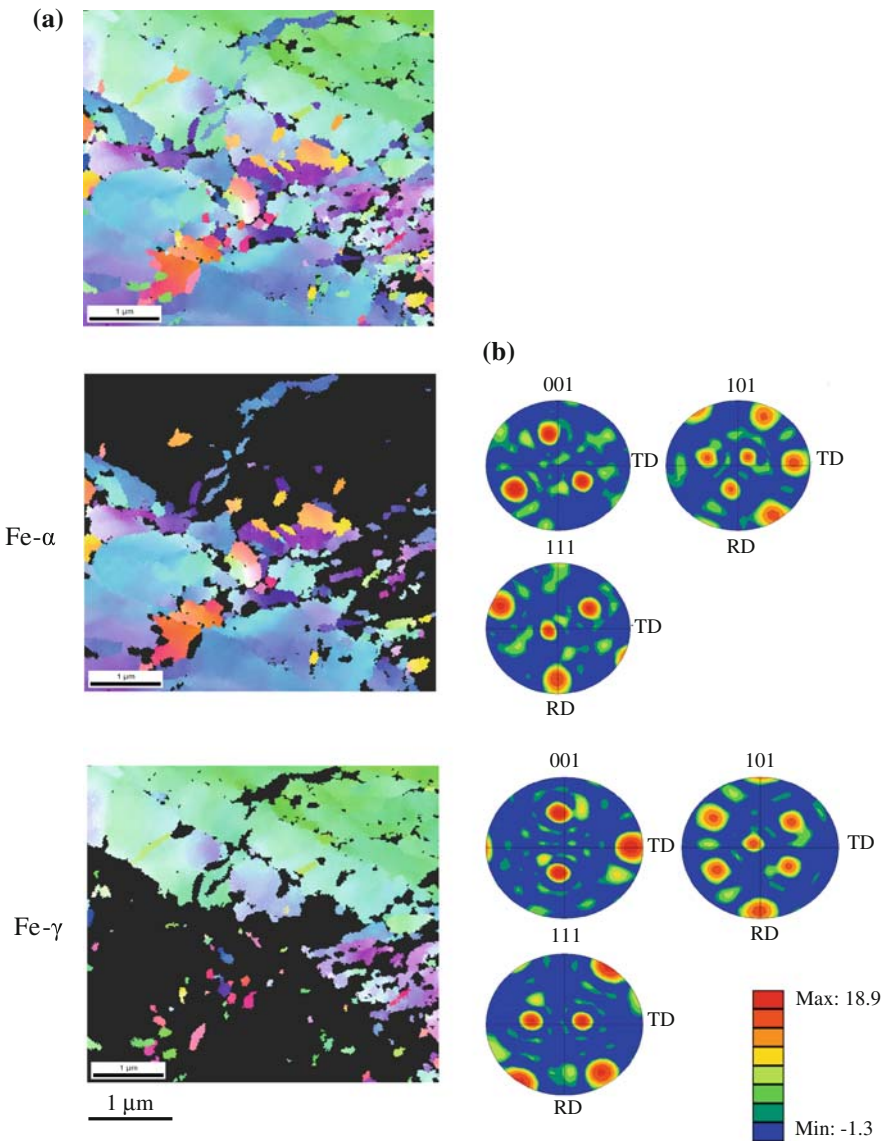

Fig. 7 EBSD analysis of deformed zone in Sample A **a** crystal orientation map and **b** the (001), (100), and (110) pole figures, showing Fe-α and Fe-γ phases, respectively

in Sample D (Fig. 5b), small grains with many nano-sized particles are observed, as indicated by the arrows. Such particles might be related to the carbide, which precipitated by the high temperature heating. Figure 6 displays the SEM images of the microstructure, crystal-orientation maps, and phase map obtained by EBSD analysis in Samples A and D. The color level of each pixel in the crystal-orientation map is defined according to the deviation of the measured orientation from the direction parallel to ND (see the color key of the stereographic projection). From the EBSD analysis in Fig. 6a, randomly oriented crystals in large grains with 6.02 μm in diameter are clearly observed in the undeformed zone of Sample A. The sample also displays a strong texture characteristic of Fe-γ, in which the total fraction of Fe-γ is 98% (Fe-α = 2%). On the other hand, the crystal orientation in the deformed zone of Sample A is complicated due to share bands, as seen in Fig. 6b. The average grain size of the deformed zone is 0.92 μm and the phase texture of Fe-α and Fe-γ is almost same level: Fe-α = 58% and Fe-γ = 42%. The increment of Fe-α phase would be attributed to the strain-induced martensite formation. It is well known that the plastic deformation of austenite can induce martensitic transformation in Fe-based alloys. It should be pointed out that the area, observed in Fig. 6b, can be deformed greatly by the compressive applied load, but the phase texture in the related region has not been altered completely to Fe-α. The reason behind this might be related to the different dislocation density [20, 21]. Details of phase formation (Fe-α and Fe-γ) in the deformed zone can be further observed in Fig. 7, in which several slip bands and changed phase formation is clarified. The microstructure in the deformed zone for Sample D shows recrystallized small grains (Fig. 6c). In this case, the grain size is found to be 1.86 μm,

and the total fraction of Fe-γ phase is recovered to 97% (Fe-α = 3%). It is also observed in Fig. 6c that many black points and tiny black islands are obtained as indicated by the arrows, which could be caused by either carbide precipitation or strain by slip band. From this result, it can be briefly concluded that the plastic deformation zone in stainless steel can be identified even at low magnification because of the varying microstructural characteristic in the plastic zone, e.g., random crystal orientation, recrystallized small grains, and precipitated nano-size particles.

Conclusions

An etching technique for revealing the plastic deformation zone in a SUS303 stainless steel has been studied experimentally and numerically. The following conclusions can be drawn.

(1) With the proposed etching technique, the localized plastic deformation in the SUS303 stainless steel sample can be revealed clearly. The procedure of the etching technique is summarized as follows: (i) the specimens are plastically strained by applied compressive stress, (ii) the strained samples are heated to various temperatures before grinding to a mirror level, (iii) the polished surface is then etched for 30 s using an etchant consisting of 5-g $FeCl_3$, 50-mL HCl, and 100-mL H_2O.

(2) The sample in the plastic deformation zone can be seen as a bright region although a dark area in the undeformed area. From the discoloration, the plastic deformation zone can be observed even on the macro scale. As revealed, the profile of the plastic deformation zone revealed by the etching technique was in good agreement with the results of the von-Mises plastic strain distribution obtained by finite element analysis.

(3) With the EBSD analysis, microstructural characteristics, such as grain orientation and phase texture, in the un- and deformed zones were clarified. Large grains of Fe-γ phase with 6.02 μm in diameter are obtained in the undeformed zone, whereas small grain with 0.92 μm is detected in the deformed zone, in which the phase texture of Fe-α and Fe-γ is almost same level. The increment of Fe-α would be caused by the strain-induced martensite formation. The amount of Fe-γ phase in the deformed zone is recovered to be 97% by the heating process.

(4) The plastic deformation zone in the stainless steel as revealed in this way corresponds to a change of microstructural characteristics. The microstructure in the plastically deformed zone is altered in different ways: the formation of randomly oriented crystals, the recrystallization of small grains, and precipitated nano-size particles.

Acknowledgements This study was financially supported by Amada Foundation for Metal Work Technology in Japan. The authors would like to appreciate experimental support by Mr. K. Funatsu at Foundation for Promotion of Material Science and Technology of Japan.

References

1. Fry A (1921) Stahl Eisen 41:1093
2. Morris CE (1949) Metal Progress 56:696
3. Hundy BB (1954) Metallurgia 49:109
4. Green AP, Hundy BB (1956) J Mech Phys Solids 4:128
5. Green AP (1956) J Mech Phys Solids 4:259
6. Birol Y (1988) Metallography 21:77
7. Frühauf J, Gärtner E, Jänsch E (1999) Appl Phys A 68:673
8. Meguid SA (1978) Metallography 11:211
9. Tucker CM (1930) Met Alloys 1:655
10. Okayasu M, Wang Z, Chen DL (2005) Mater Sci Technol 21:530
11. Okayasu M, Sato K, Mizuno M (2008) J Mater Sci 43:2792. doi: 10.1007/s10853-008-2544-y
12. Okayasu M, Shin DH, Mizuno M (2008) Mater Sci Eng A 474:140
13. Okayasu M, Sato K, Mizuno M (2010) Mater Sci Technol (in press)
14. Wu X, Pan X, Mabon JC, Li M, Stubbins JF (2006) J Nucl Mater 356:70
15. Jia N, Peng RL, Chai GC, Johansson S, Wang YD (2008) Mater Sci Eng A 491:425
16. Chen X, Wang Y, Gong M, Xia Y (2004) J Mater Sci 39:4869. doi:10.1023/B:JMSC.0000035327.55210.99
17. Randle V (2003) Microtexture determination and its applications, 2nd edn. Money, London
18. ANSYS Inc. (1999) ANSYS Contact technology guide
19. Talonen J, Hanninen H (2007) Acta Mater 55:6108
20. Durlu TN (1992) J Mater Sci Lett 11:702
21. Youliang HE, Stéphane G, Pascal JJ, John JJ (2006) Metall Mater Trans A 37:2641